

## New Lanthanide Silicates Based on Anionic Silicate Chain, Layer, and Framework Prepared under High-Temperature and High-Pressure Conditions

Xinguang Zhao, Jiyang Li, Peng Chen, Yi Li, Qingxin Chu, Xiaoyang Liu,\* Jihong Yu,\* and Ruren Xu

State Key Laboratory of Inorganic Synthesis and Preparative Chemistry, College of Chemistry, Jilin University, Changchun 130012, P. R. China

Received March 31, 2010

Three new lanthanide silicates  $K_{1.25}Gd_{1.25}Si_{2.5}O_{7.5}$  (denoted as GdSiO-CJ7),  $Cs_3TbSi_6O_{19} \cdot 2H_2O$  (denoted as TbSiO-CJ8), and  $Cs_3DySi_6O_{15}$  (denoted as DySiO-CJ9) were synthesized by using a high-temperature and high-pressure hydrothermal method. Their structures determined by single-crystal X-ray diffraction revealed anionic silicate chain, layer and framework, which are further connected with  $LnO_n$  polyhedra to form novel lanthanide silicate frameworks. The structure of GdSiO-CJ7 consists of unbranched silicate chains  $[Si_5O_{15}]^{10-}$  extending along the *b* axis, which are linked together by edge-sharing linked  $GdO_6$  and  $GdO_8$  chains along the *c* axis to form a 3-D framework with two types of 10-ring channels along the [010] and [001] directions, respectively. The structure of TbSiO-CJ8 consists of double 4,8-net sheets  $[Si_8O_{19}]^{6-}$  built up from  $SiO_4$  tetrahedra, which are linked together via  $TbO_6$  octahedra to form a 3-D framework with 8-ring channels along the [100] and [010] directions. The structure of DySiO-CJ9 is based on a 3-D silicate framework  $[Si_6O_{15}]^{6-}$  with 6-rings, where  $DyO_6$  octahedra are located between two adjacent 6-rings and connected with six Si atoms via O atoms. The photoluminescence photoluminescence properties of TbSiO-CJ8 and EuSiO-CJ8 were investigated.

### Introduction

Microporous metal silicates constitute an important class of materials because of their uniform microporosity, high thermal stability and technological importance in applications

such as catalysis, ion-exchange and separation.<sup>1,2</sup> A large number of main group elements,<sup>3–6</sup> transition metals,<sup>7–17</sup> lanthanide elements,<sup>18–29</sup> and uranium<sup>30–35</sup>-based silicates

\*To whom correspondence should be addressed. E-mail: jihong@jlu.edu.cn (J.Y.); liuxy@jlu.edu.cn (X.L.). Tel & Fax: +86-431-85168608 (J.Y.); +86-431-85168316 (X.L.).

- (1) Shannon, R. D.; Taylor, B. E.; Gier, T. E.; Chen, H. Y.; Berzins, T. *Inorg. Chem.* **1978**, *17*, 958.
- (2) Rocha, J.; Carlos, L. D. *Curr. Opin. Solid State Mater. Sci.* **2003**, *7*, 199.
- (3) Ferreira, A.; Lin, Z.; Rocha, J.; Morais, C. M.; Lopes, M.; Fernandez, C. *Inorg. Chem.* **2001**, *40*, 3330.
- (4) Ferreira, A.; Lin, Z.; Soares, M. R.; Rocha, J. *Inorg. Chim. Acta* **2003**, *356*, 19.
- (5) Huang, L. I.; Wang, S. L.; Szu, S. P.; Hsieh, C. Y.; Kao, H. M.; Lii, K. H. *Chem. Mater.* **2004**, *16*, 1660.
- (6) Huang, L. I.; Wang, S. L.; Chen, C. Y.; Chang, B. C.; Lii, K. H. *Inorg. Chem.* **2005**, *44*, 2992.
- (7) Wang, X.; Liu, L.; Jacobson, A. J. *Angew. Chem., Int. Ed.* **2001**, *40*, 2174.
- (8) Wang, X.; Liu, L.; Jacobson, A. J. *J. Am. Chem. Soc.* **2002**, *124*, 7812.
- (9) Brandaõ, P.; Valente, A.; Philippou, A.; Ferreira, A.; Anderson, M. W.; Rocha, J. *Eur. J. Inorg. Chem.* **2003**, 1175.
- (10) Nyman, M.; Bonhomme, F.; Teter, D. M.; Maxwell, R. S.; Bu, B. X.; Wang, L. M.; Ewing, R. C.; Nenoff, T. M. *Chem. Mater.* **2000**, *12*, 3449.
- (11) Nyman, M.; Bonhomme, F.; Maxwell, R. S.; Nenoff, T. M. *Chem. Mater.* **2001**, *13*, 4603.
- (12) Francis, R. J.; Jacobson, A. J. *Angew. Chem., Int. Ed.* **2001**, *40*, 2879.
- (13) Kao, H. M.; Lii, K. H. *Inorg. Chem.* **2002**, *41*, 5644.
- (14) Li, C. Y.; Hsieh, C. Y.; Lin, H. M.; Kao, H. M.; Lii, K. H. *Inorg. Chem.* **2002**, *41*, 4206.
- (15) Hung, L. I.; Wang, S. L.; Kao, H. M.; Lii, K. H. *Inorg. Chem.* **2003**, *42*, 4057–4061.
- (16) Hung, L. I.; Wang, S. L.; Szu, S. P.; Hsieh, C. Y.; Kao, H. M.; Lii, K. H. *Chem. Mater.* **2004**, *16*, 1660–1666.

- (17) Lo, F. R.; Lii, K. H. *J. Solid State Chem.* **2005**, *178*, 1017.
- (18) Ananias, D.; Ferreira, A.; Rocha, J.; Ferreira, P.; Rainho, J. P.; Morais, C.; Carlos, L. D. *J. Am. Chem. Soc.* **2001**, *123*, 5735.
- (19) Ferreira, A.; Ananias, D.; Carlos, L. D.; Morais, C. M.; Rocha, J. *J. Am. Chem. Soc.* **2003**, *125*, 14573.
- (20) Rocha, J.; Ferreira, P.; Carlos, L. D.; Ferreira, A. *Angew. Chem., Int. Ed.* **2000**, *39*, 3276.
- (21) Jeong, H. K.; Chandrasekaran, A.; Tsapatsis, M. *Chem. Commun.* **2002**, 2398.
- (22) Haile, S. M.; Wuensch, B. J. *Acta Crystallogr.* **2000**, *B56*, 335.
- (23) Haile, S. M.; Wuensch, B. J. *Acta Crystallogr.* **2000**, *B56*, 349.
- (24) Huang, M. Y.; Chen, Y. H.; Chang, B. C.; Lii, K. H. *Chem. Mater.* **2005**, *17*, 5743.
- (25) Wang, G.; Li, J.; Yu, J.; Chen, P.; Pan, Q.; Song, H.; Xu, R. *Chem. Mater.* **2006**, *18*, 5637.
- (26) Wang, G. M.; Yan, W. F.; Chen, P.; Wang, X.; Qian, K.; Su, T.; Yu, J. H. *Microporous Mesoporous Mater.* **2007**, *105*, 58.
- (27) Kowalchuk, C. M.; Paz, F. A. A.; Ananias, D.; Pattison, P.; Carlos, L. D.; Rocha, J. *J. Chem.—Eur. J.* **2008**, *14*, 8157.
- (28) Ananias, D.; Kostova, M.; Paz, F. A. A.; Ferreira, A.; Carlos, L. D.; Klinowski, J.; Rocha, J. *J. Am. Chem. Soc.* **2004**, *126*, 10410.
- (29) Kostova, M. H.; Ananias, D.; Paz, F. A. A.; Ferreira, A.; Rocha, J.; Carlos, L. D. *J. Phys. Chem. B* **2007**, *111*, 3576.
- (30) Wang, X.; Huang, J.; Jacobson, A. J. *J. Am. Chem. Soc.* **2002**, *124*, 15190.
- (31) Huang, J.; Wang, X.; Jacobson, A. J. *J. Mater. Chem.* **2003**, *13*, 191.
- (32) Burns, P. C.; Olson, R. A.; Finch, R. J.; Hanchar, J. M.; Thibault, Y. *J. Nucl. Mater.* **2000**, *278*, 290.
- (33) Chen, C. S.; Kao, H. M.; Lii, K. H. *Inorg. Chem.* **2005**, *44*, 935.
- (34) Chen, C. S.; Chiang, R. K.; Kao, H. M.; Lii, K. H. *Inorg. Chem.* **2005**, *44*, 3914.
- (35) Chen, C. S.; Lee, S. F.; Lii, K. H. *J. Am. Chem. Soc.* **2005**, *127*, 12208.

have been synthesized. Most of these compounds were synthesized under mild hydrothermal conditions in Teflon-lined stainless steel autoclaves in the temperature range of 100–240 °C. Recently, a lot of research has been focused on the synthesis of metal silicates under high-temperature and high-pressure conditions. High pressure in the synthetic chemistry can play two important roles: first, decreasing the interatomic distances in existing materials; second, synthesizing of new materials through the densification effect, the stabilization of the precursors, the compressing of the corresponding atoms and improvement of the reactivity.<sup>36</sup> For examples, Harrison et al. reported a titanosilicate  $\text{Cs}_3\text{HTi}_4\text{O}_4(\text{SiO}_4)_3 \cdot 4\text{H}_2\text{O}$  synthesized at 750 °C and 200 MPa in 1995.<sup>37</sup> Lii and his research group have done extensive work in this field, since 2002. They have synthesized a series of metal silicates, including niobium silicates,<sup>13</sup> vanadium silicates,<sup>14</sup> indium silicates,<sup>15,16</sup> stannosilicates,<sup>17</sup> and uranium silicates<sup>33–35</sup> by means of high temperature and high pressure method.

In recent decades, many studies were expanded to the lanthanide silicates because of their high thermal stability and interesting luminescent properties. In 2000, the first cerium silicate AV-5 was reported by Rocha and co-workers under mild hydrothermal conditions at 503K.<sup>20</sup> Later on, they reported a series of lanthanide silicates including AV-9 (Ln = Eu, Tb, Er),<sup>18</sup> AV-20 (Ln = Ce, Sm, Eu, Tb),<sup>19</sup> AV-21 (Ln = La, Sm, Eu, Gd, Tb),<sup>27</sup> AV-22 (Ln = Eu, Gd, Tb, Er),<sup>28</sup> and AV-23 (Ln = Y, Eu, Tb, Er).<sup>29</sup> In 2002, Jeong et al. reported a hydrothermally synthesized lanthanide silicate  $\text{Na}_{4.8}\text{Ce}_2\text{Si}_{12}\text{O}_{30}$  with 8-ring channels.<sup>21</sup> Recently, our research group reported two microporous lanthanide silicates TbSiO-CJ1 containing helical sechser (six) silicate chains and 9-ring channels<sup>25</sup> and CeSiO-CJ2 containing mixed valence of cerium  $\text{Ce}^{\text{III}}/\text{Ce}^{\text{IV}}$ .<sup>26</sup> However, the reports of lanthanide silicates synthesized under high-temperature and high-pressure conditions are limited. In 1993, Haile and co-workers first used high-temperature and high-pressure technique in the hydrothermal synthesis and successfully prepared a number of neodymium and yttrium silicates to search for fast alkali ion conductors.<sup>38,39</sup> In 2005, Lii and co-workers reported a new europium silicate  $\text{Cs}_3\text{EuSi}_6\text{O}_{15}$  synthesized at 600 °C and 170 MPa, and investigated its crystal structure as well as luminescence properties.<sup>24</sup> Generally, these compounds can not be obtained under mild hydrothermal conditions.

In this work, we employed the high-temperature and high-pressure hydrothermal synthetic method to successfully synthesize three new types of lanthanide silicates  $\text{K}_{1.25}\text{Gd}_{1.25}\text{Si}_{2.5}\text{O}_{7.5}$  (GdSiO-CJ7),  $\text{Cs}_3\text{TbSi}_8\text{O}_{19} \cdot 2\text{H}_2\text{O}$  (TbSiO-CJ8), and  $\text{Cs}_3\text{DySi}_6\text{O}_{15}$  (DySiO-CJ9). GdSiO-CJ7 and TbSiO-CJ8 have 10- and 8-ring channels, respectively, while DySiO-CJ9 has only 6-rings. The photoluminescence properties of TbSiO-CJ8 and EuSiO-CJ8 have been investigated.

## Experimental Section

Under high-temperature and high-pressure conditions, three new lanthanide silicates were synthesized by varying the rare-earth elements, the cations, the temperature and the reaction time.

**Synthesis of  $\text{K}_{1.25}\text{Gd}_{1.25}\text{Si}_{2.5}\text{O}_{7.5}$  (GdSiO-CJ7).** GdSiO-CJ7 was synthesized from the reaction mixture of 0.301 g of KOH, 0.15 g of  $\text{GdCl}_3 \cdot 6\text{H}_2\text{O}$ , 0.097 g of fumed silica (molar ratio K/Gd/Si = 6.67:1:4), and 400  $\mu\text{L}$  of water in a 7 cm long copper tube (inside diameter = 4 mm). The sealed copper tube and 75 mL of distilled water were put in the NIKKISO autoclave and heated at 400 °C for 14 days. The pressure was estimated to be 80 MPa according to the pressure–temperature diagram of pure water. Then the autoclave was taken out of the furnace and cooled to room temperature by natural cooling. The resulting cubic-shaped colorless crystals with some amorphous phase were washed with distilled water and dried in air at 60 °C.

**Synthesis of  $\text{Cs}_3\text{TbSi}_8\text{O}_{19} \cdot 2\text{H}_2\text{O}$  (TbSiO-CJ8).** TbSiO-CJ8 was synthesized under high-temperature and high-pressure hydrothermal conditions. The reactions were carried out in a platinum ampule contained in a Leco Tem-Pre autoclave under autogenous pressure. Typically, a reaction mixture of 466  $\mu\text{L}$   $\text{CsOH}_{(\text{aq})}$  (50 wt %,  $d = 1.72 \text{ g/mL}$ ), 0.05 g of  $\text{Tb}_4\text{O}_7$ , and 0.0964 g of fumed silica (molar ratio Cs/Tb/Si = 10:1:6) was sealed in a 2 cm long platinum ampule (inside diameter = 3 mm) with a little amount of water (about 80  $\mu\text{L}$ ). Then the sealed platinum ampule and 15 mL distilled water were put in the Leco autoclave and heated at 600 °C for three days. The filling percentage of the autoclave by distilled water at room temperature was 65%. The pressure was estimated to be 220 MPa according to the pressure–temperature diagram of pure water. After the reaction, the autoclave was cooled to 400 °C at a rate of 2 °C/h, followed by removing the autoclave from the furnace to fast cooling to room temperature. The product containing colorless short-rod crystals mixed with some amorphous phase was washed with distilled water and dried in the air at 60 °C.

Pure powder phase of TbSiO-CJ8 could be synthesized under mild hydrothermal conditions. Typically, 0.521 g of  $\text{CsOH}_{(\text{aq})}$  (50 wt %) and 0.052 g  $\text{SiO}_2$  were first dissolved in 2.0 mL of deionized water. Then 0.05 g  $\text{Tb}(\text{NO}_3)_3 \cdot 6\text{H}_2\text{O}$  was subsequently added. The resulting mixture has a molar ratio of  $\text{CsOH}/\text{Tb}(\text{NO}_3)_3/\text{SiO}_2/\text{H}_2\text{O} = 12:1:6:1000$ . After the mixture was continuously stirred for 1 h, the homogeneous gel was loaded in a Teflon-lined stainless steel autoclave (15 mL). The reaction was conducted at 230 °C for 14 days under static condition. Under the similar reaction conditions, using  $\text{Eu}(\text{NO}_3)_3 \cdot 6\text{H}_2\text{O}$  instead of  $\text{Tb}(\text{NO}_3)_3 \cdot 6\text{H}_2\text{O}$ , could give rise to the analogous europium silicate (denoted as EuSiO-CJ8).

**Synthesis of  $\text{Cs}_3\text{DySi}_6\text{O}_{15}$  (DySiO-CJ9).** The synthesis conditions of DySiO-CJ9 were similar to those of TbSiO-CJ8, except for using  $\text{Dy}_2\text{O}_3$  instead of  $\text{Tb}_4\text{O}_7$  as the raw material. The starting materials were 385  $\mu\text{L}$   $\text{CsOH}_{(\text{aq})}$  (50 wt %,  $d = 1.72 \text{ g/mL}$ ), 0.04 g of  $\text{Dy}_2\text{O}_3$ , and 0.0663 g of fumed silica, and the molar ratio of Cs/Dy/Si was 10:1:5. The reaction produced stick-shaped colorless crystals and some amorphous phase.

**Characterizations.** The X-ray powder diffraction (XPRD) was performed on Rigaku D/max 2550 X-ray diffractometer. Inductively coupled plasma (ICP) analysis was performed on a Perkin-Elmer Optima 3300 DV ICP instrument. The TGA was carried out on a Perkin-Elmer TGA-7 thermogravimetric analyzer in the air with a heating rate of 10 °C/min. The photoluminescence measurement was performed on F-4500 FL Spectrophotometer.

Suitable single crystals of GdSiO-CJ7, TbSiO-CJ8 and DySiO-CJ9 with dimensions of  $0.10 \times 0.10 \times 0.08 \text{ mm}^3$ ,  $0.15 \times 0.12 \times 0.10 \text{ mm}^3$  and  $0.12 \times 0.10 \times 0.08 \text{ mm}^3$ , respectively, were selected for single-crystal X-ray diffraction analysis. Intensity data collection and structure analysis were performed on a Bruker SMART CCD diffractometer using graphite-monochromated Mo K $\alpha$  radiation ( $\lambda = 0.71073 \text{ \AA}$ ) at room temperature. Data processing was accomplished with the SAINT processing program. The structures were solved by direct methods and refined by on F<sup>2</sup> by full-matrix least-squares techniques using SHELXTL crystallographic program package. These three structures were solved in the space group *Cmme*, *Pnma*, and *R $\bar{3}m$* , respectively. Empirical absorption correction was

(36) Demazeau, G. *J. Phys.: Condens. Matter* **2002**, *14*, 11031.

(37) Harrison, W. T. A.; Gier, T. E.; Stucky, G. D. *Zeolite* **1995**, *15*, 408.

(38) Haile, S. M.; Wuensch, B. J.; Siegrist, T.; Laudise, R. A. *J. Cryst. Growth* **1993**, *131*, 352.

(39) Haile, S. M.; Wuensch, B. J.; Laudise, R. A. *J. Cryst. Growth* **1993**, *131*, 373.

**Table 1.** Crystal Data and Structure Refinement Parameters of These Three Compounds

identification code	GdSiO-CJ7	TbSiO-CJ8	DySiO-CJ9
empirical formula	$K_{1.25}Gd_{1.25}Si_{2.5}O_{7.5}$	$H_2Cs_{1.5}Tb_{0.5}Si_4O_{10.5}$	$Cs_{0.25}Dy_{0.08}Si_{10.5}O_{1.25}$
formula weight	435.66	561.20	80.81
temperature (K)	293(2)	293(2)	296(2)
wavelength (Å)	0.71073	0.71073	0.71073
space group	<i>Cmme</i>	<i>Pnma</i>	$R\bar{3}m$
<i>a</i> (Å)	21.853(4)	11.5208(3)	13.9959(12)
<i>b</i> (Å)	22.857(5)	7.0607(2)	13.9959(12)
<i>c</i> (Å)	6.5543(13)	27.0430(8)	7.1775(6)
vol (Å <sup>3</sup> )	3273.8(11)	2199.81(11)	1217.60(18)
<i>Z</i>	16	8	36
<i>D</i> <sub>calcd</sub> (g/cm <sup>3</sup> )	3.536	3.389	3.968
abs coeff (mm <sup>-1</sup> )	11.097	8.638	11.750
$\theta$ range	1.86–28.22°	1.92–28.27°	2.91–28.14°
goodness-of-fit on <i>F</i> <sup>2</sup>	1.058	1.053	1.242
final <i>R</i> indices [ <i>I</i> > 2 $\sigma$ ( <i>I</i> )] <sup>a</sup>	<i>R</i> <sub>1</sub> = 0.0358 <i>R</i> <sub>2</sub> = 0.1066	<i>R</i> <sub>1</sub> = 0.0425 <i>R</i> <sub>2</sub> = 0.1086	<i>R</i> <sub>1</sub> = 0.0327 <i>R</i> <sub>2</sub> = 0.0796
<i>R</i> indices (all data) <sup>a</sup>	<i>R</i> <sub>1</sub> = 0.0435 <i>R</i> <sub>2</sub> = 0.1105	<i>R</i> <sub>1</sub> = 0.0509 <i>R</i> <sub>2</sub> = 0.1136	<i>R</i> <sub>1</sub> = 0.0331 <i>R</i> <sub>2</sub> = 0.0799

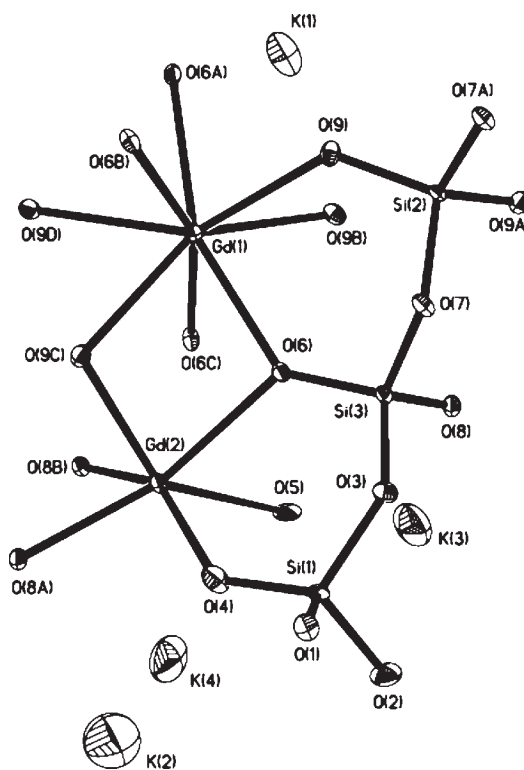
$$^a R_1 = \Sigma(\Delta F/\Sigma(F_0)); R_2 = (\Sigma[w(F_0^2 - F_c^2)])/\Sigma[w(F_0^2)^{1/2}]; w = 1/\sigma^2(F_0^2).$$

applied for all these three structures. All heaviest atoms, Gd, K, and Si for GdSiO-CJ7, Tb, Cs, and Si for TbSiO-CJ8, and Dy, Cs, and Si for DySiO-CJ9, were located, and then O atoms were found in the subsequent difference Fourier maps. For GdSiO-CJ7, the occupancy factors of both K(3) and K(4) were set to 0.125 in order to balance the charge of the framework [Gd<sub>1.25</sub>Si<sub>2.5</sub>O<sub>7.5</sub>]<sup>1,25-</sup>. ICP analysis for some picked single crystals from the batch product of GdSiO-CJ7 was consistent with empirical formula given by single-crystal analysis (Gd, expt. 44.8 wt % and calcd. 45.1 wt %; K, expt. 10.9 wt % and calcd. 11.2 wt %). For TbSiO-CJ8, the occupancy factors of Cs(3) and Cs(3') were set as 0.1 and 0.4, respectively, to balance the charge of the framework which was consistent with their electron densities in the difference Fourier map. For DySiO-CJ9, all Si, O, and Cs atoms are positionally disordered. No hydrogen atoms were found but added geometrically. All non-hydrogen atoms were refined anisotropically. Experimental details for the structural determination are listed in Table 1.

## Result and Discussion

**Crystallization Conditions.** Large single crystals of these three compounds could be only obtained under rigorous high-temperature and high-pressure hydrothermal conditions. Powder phases of TbSiO-CJ8 and EuSiO-CJ8 could be synthesized under mild hydrothermal conditions at 230 °C, their phase purity has been confirmed by powder XRD patterns of newly synthesized samples as compared with the simulated one based on single-crystal structure analysis (Figure S1, Supporting Information). However, no GdSiO-CJ7 and DySiO-CJ9 crystalline phases were formed under mild hydrothermal conditions, but only amorphous phases.

For TbSiO-CJ8 and DySiO-CJ9, it was found that the cooling process played an important role in the crystallization. If the temperature was decreased to room temperature by quenching or natural cooling after the reaction, the products were not crystallized or the degree of crystallinity was poor. However, if the cooling process is 2 °C/h down to room temperature, the crystals were not perfect enough. Through a series of experiments, we found that the best cooling process was to cool the autoclave to 400 at 2 °C/h followed by fast cooling to room temperature. As for GdSiO-CJ7, it was prepared at a lower temperature, i.e., 400 °C and therefore, the influence of the cooling process was not obvious.

**Figure 1.** Thermal ellipsoid plot (50%) of GdSiO-CJ7.

**Single-Crystal Structure of GdSiO-CJ7.** GdSiO-CJ7 crystallizes in the space group *Cmme* (No. 67) with *a* = 21.853(4) Å, *b* = 22.857(5) Å, and *c* = 6.5543(13) Å. The asymmetric unit of GdSiO-CJ7 contains two symmetrically independent Gd sites, three symmetrically independent Si sites, four symmetrically independent K sites as shown in Figure 1. All of the Si sites are in 4-fold coordination to O atoms in tetrahedral geometry. The atoms in Si(2) and Si(3) sites are connected with two Si atoms and two Gd atoms via bridging O atoms, while the atoms in Si(1) site is connected with three Si atoms and one Gd atom via bridging O atoms. Of the two independent Gd sites, the atom in Gd(1) site is coordinated to eight O atoms forming an antiprismatic square polyhedron and sits on the intersection point of three 2-fold axes

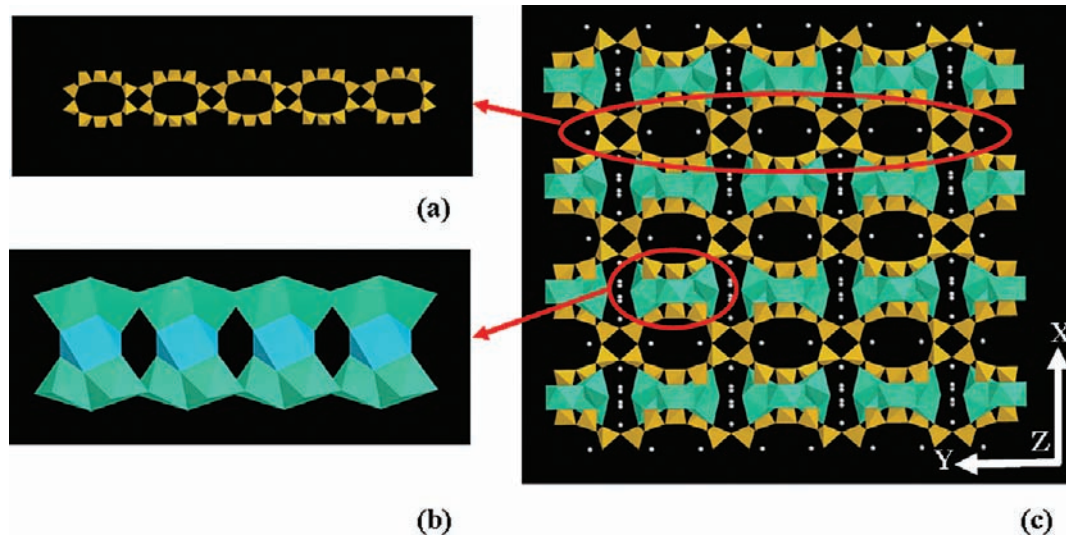


**Figure 2.** (a) Zigzag silicate chains with 4- and 10-rings along [010] direction; (b) Gd chains made up of edge-sharing GdO<sub>6</sub> and GdO<sub>8</sub> polyhedra along [001] direction; (c) polyhedral view of the open-framework structure of GdSiO-CJ7 contains 10-ring channels along [001] direction (Cyan, Gd; yellow, Si; white, K).

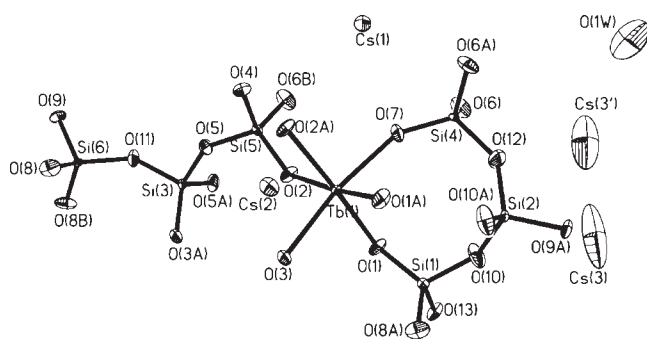


**Figure 3.** Thermal ellipsoid plot (50%) of TbSiO-CJ8.

(Wyckoff position 4a). The atom in Gd(2) site is connected to five Si atoms and one Gd atom via bridging O atoms to form GdO<sub>6</sub> octahedron. Among all O sites, O(6), O(8) and O(9) are the  $\mu_3$ -O atoms. The observed Si–O bond lengths of 1.568–1.671 Å and O–Si–O bond angles of 103.9–123.0° are of typical of silicate materials. The Gd–O bond lengths and O–Gd–O bond angles are in the range of 2.261–2.504 Å and 65.8–156.4°, respectively. All of the four K sites are situated on the mirror plane (Wyckoff position 8 m, 8n, 8n and 8n, respectively). The occupancy factors of both K(3) and K(4) are set to 0.125 to balance the charge of the framework.

As shown in Figure 2, the structure of GdSiO-CJ7 consists of complex zigzag silicate chains [Si<sub>5</sub>O<sub>15</sub>]<sup>10-</sup> containing 4- and 10-rings running along the [010] direction (Figure 2a). One GdO<sub>8</sub> polyhedron is connected with four GdO<sub>6</sub> octahedra via edge-sharing connection to form a cluster. Such clusters are linked together by Gd–O–Gd bonds to form an infinite chain along the [001] direction (Figure 2b). The silicate chains that are made up from SiO<sub>4</sub> tetrahedra and gadolinium chains made up from GdO<sub>6</sub> and GdO<sub>8</sub> polyhedra are arranged in parallel directions along [010] and [001], respectively, and further connected by Gd–O–Si bonds to form the 3-D framework of GdSiO-CJ7 (Figure 2c). The structure contains 8-ring channels along the [001] direction and two kinds of 10-ring channels along the [010] and [001] directions, respectively. K(1) is located in the 10-ring channels, while

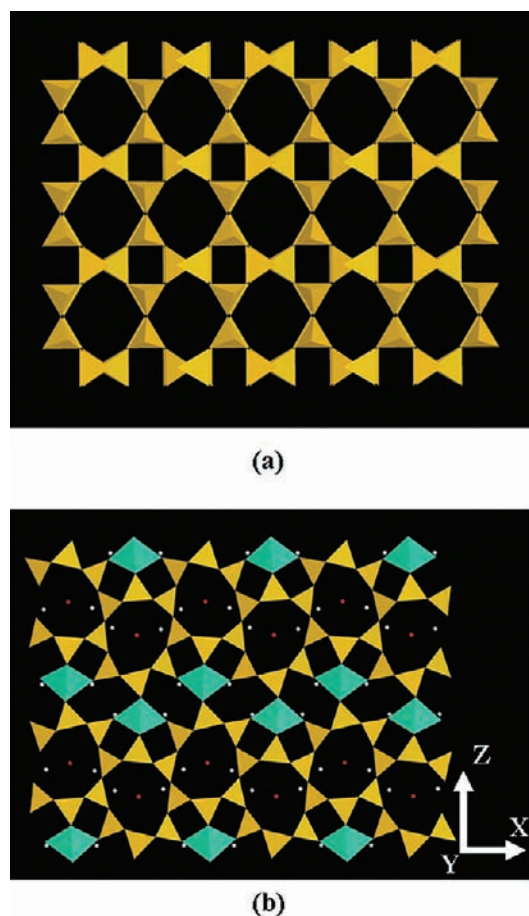


**Figure 4.** (a) Undulated silicate double layers containing 4- and 8-rings; (b) polyhedral view of the open-framework structure of TbSiO-CJ8 along [010] direction (cyan, Tb; yellow, Si; white, Cs; red, O).

K(2), K(3) and K(4) are located between the gadolinium chains. So far, the reported lanthanide silicates have been found with 8-, 9-, and 12-ring channels, but the 10-ring channel in GdSiO-CJ7 is first observed in lanthanide silicates.

**Single-Crystal Structure of TbSiO-CJ8.** TbSiO-CJ8 crystallizes in the space group *Pnma* (No. 62) with

$a = 11.5208(3) \text{ \AA}$ ,  $b = 7.0607(2) \text{ \AA}$ , and  $c = 27.0430(8) \text{ \AA}$ . The asymmetric unit of TbSiO-CJ8 contains one symmetrically independent Tb site, six symmetrically independent Si sites, and four symmetrically independent Cs sites as shown in Figure 3. All six distinct Si sites are in tetrahedra environments, in which the Si atoms in Si(1), Si(3), Si(4) and Si(5) sites are connected to three Si atoms and one Tb atom via bridging O atoms, while the Si atoms in Si(2) and Si(6) sites are connected to four Si atoms via bridging O atoms. Si(2), Si(3), Si(4), and Si(6) sites are on the mirror planes (Wyckoff position  $4c$ ), while Si(1) and Si(5) sites are in the general sites. The observed Si–O bond lengths in the range of 1.561–1.641 Å and O–Si–O bond angles in the range of 103.4–115.6° are typical values within the normal range according to the reported work.<sup>40</sup> The Tb site, located on a mirror plane (Wyckoff position  $4c$ ), is coordinated to six bridging O atoms with the adjacent Si atoms. The Tb–O bond lengths are in the range of 2.274–2.284 Å, and the O–Tb–O bond angles vary from 85.6 to 172.3°. Four symmetrically independent Cs sites are also located on the mirror planes (Wyckoff position  $4c$ ). According to the maximum cation–anion distance criterion by Donnay and Allmann,<sup>41</sup> the largest Cs–O distance is limited to 3.70 Å, therefore, the coordination number (CN) of Cs atoms are as follow: Cs(1), CN = 11; Cs(2), CN = 9; Cs(3), CN = 7; Cs(3'), CN = 9.

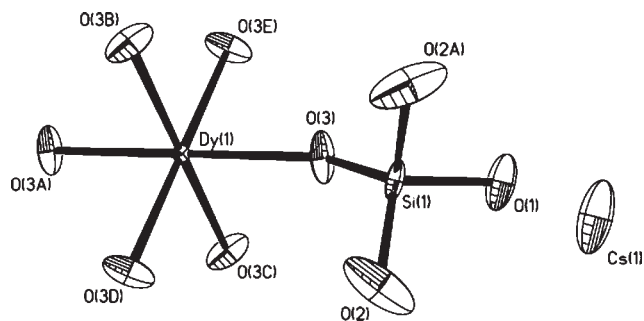


Figure 5. Thermal ellipsoid plot (50%) of DySiO-CJ9.

As shown in Figure 4, the structure of TbSiO-CJ8 consists of undulated silicate double layer with 4- and 8-rings parallel to the (001) plane, which are built up from  $\text{SiO}_4$  tetrahedra via corner sharing (Figure 4a). Such double silicate layers are linked together by  $\text{TbO}_6$  octahedra via vertex oxygen atoms resulting in a 3-D open-framework of TbSiO-CJ8 (Figure 4b). It contains 8-ring channels along the [100] and [010] directions. Cs(1) and Cs(2) cations are located near the wall of 6-ring which are delimited by four  $\text{SiO}_4$  tetrahedra and two  $\text{TbO}_6$  octahedra. Cs(3), Cs(3') and water molecules are located in the 8-ring channels. The amount of lattice water is confirmed by the TG analysis (Figure S2). TGA curve revealed a total weight loss of 3.13% from room temperature to 773 K, which is attributed to the loss of lattice water in TbSiO-CJ8 (calcd. 3.21%). TbSiO-CJ8 possesses a structure similar to that of mineral montregianite.<sup>42,43</sup> Both of them have the 4,8-net silicate layers, but the connection between the silicate layers and the lanthanide polyhedra are different.

**Single-Crystal Structure of DySiO-CJ9.** DySiO-CJ9 crystallizes in the space group  $R\bar{3}m$  (No. 166) with  $a = b = 13.9959(12) \text{ \AA}$  and  $c = 7.1775(6) \text{ \AA}$ . The asymmetric unit of DySiO-CJ9 contains one symmetrically independent Dy site, one symmetrically independent Si site and one symmetrically independent Cs site (Figure 5). The Dy site is in an octahedral environment, which is connected to six Si atoms via bridging O atoms, and located at the cross point of 3-fold rotary-inversion axis and the mirror plane (Wyckoff position  $1a$ ). The  $\text{DyO}_6$  octahedron is regular with the Dy–O bond distance of 2.233 Å. The Si site is in a tetrahedral environment, which is connected to three Si atoms and one Dy atom via bridging O atoms. The observed Si–O bond lengths are in the range of 1.556–1.633 Å and O–Si–O bond angles are in the range of 101.3–118.2°, which are typical values for silicate materials. Based on the theory of the maximum cation–anion distance, a limit of 3.70 Å was set for Cs–O interactions, which gave the coordination numbers of Cs(1) CN = 9.

As shown in Figure 6, DySiO-CJ9 possesses a 3-D silicate framework  $[\text{Si}_6\text{O}_{15}]^{6-}$  constructed from  $\text{SiO}_4$  tetrahedra

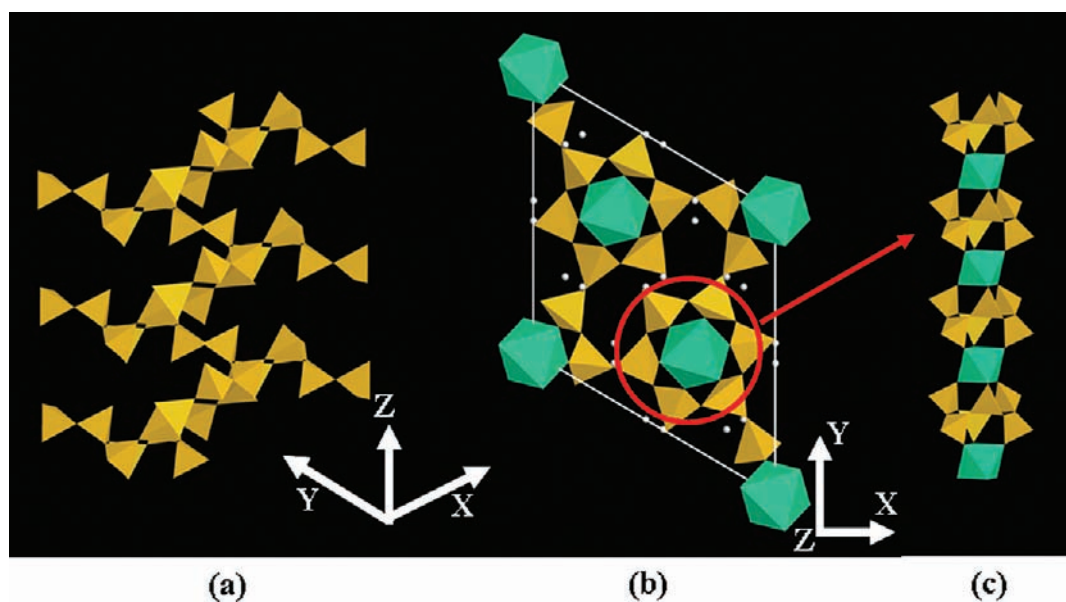
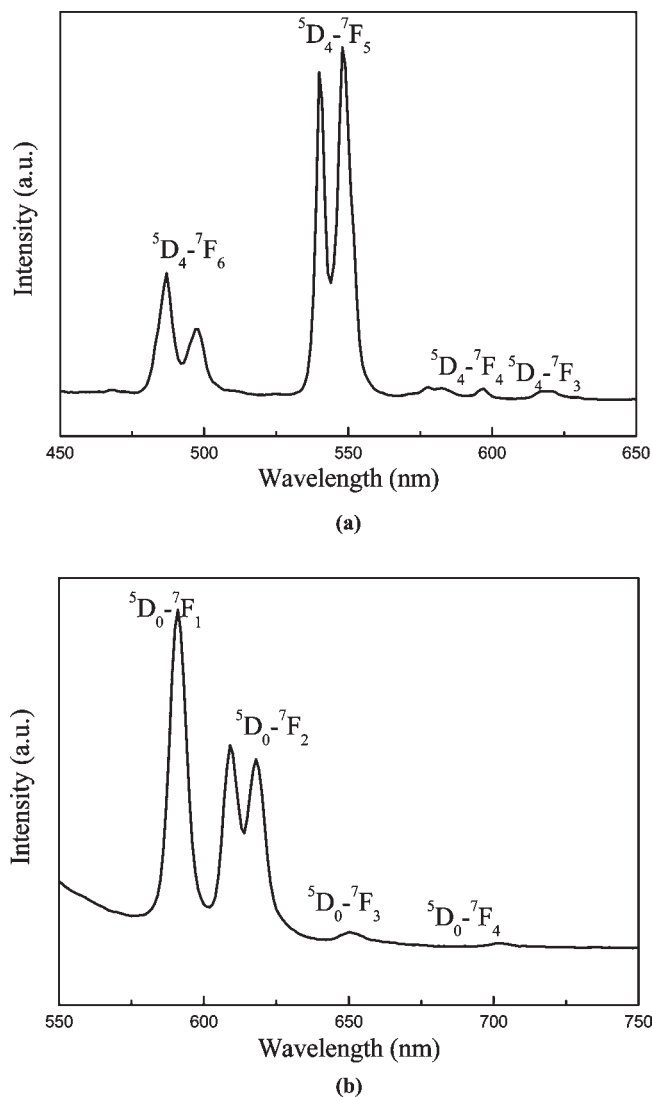


Figure 6. (a) 3-D silicate framework built up from  $\text{SiO}_4$  tetrahedra; (b) structure of DySiO-CJ9 viewed along [001] direction; (c) infinite chain along [001] direction containing D4R cages composed of six  $\text{SiO}_4$  and two  $\text{DyO}_6$  polyhedra (cyan, Dy; yellow, Si; white, Cs).



**Figure 7.** RT emission spectra of (a) TbSiO-CJ8 and (b) EuSiO-CJ8 (The  $^5D_0 \rightarrow ^7F_0$  transition is too weak which is not shown in the figure.)

(Figure 6a), which contains 6-rings along the [001] direction. The Dy atoms are located between two 6-rings to connect six Si atoms coming from two adjacent 6-rings via bridging O atoms (Figure 6b). The structure of DySiO-CJ9 can also be viewed as generated from the condensation of double-four (D4R) cages containing six Si atoms and two Dy atoms. The adjacent cages are connected via corner-sharing Dy atoms to form an infinite chain along the [001] direction (Figure 6c), which are further connected via Si–O–Si bonds to form a 3-D framework. This framework is a relatively dense phase containing only 6-rings. DySiO-CJ9 is a new silicate framework with Si/O = 2:5, which contains only tertiary  $\text{SiO}_4$  tetrahedra. Such examples are known as  $\text{Na}_{4.8}\text{Ce}_2\text{Si}_{12}\text{O}_{40} \cdot 4\text{H}_2\text{O}$ <sup>21</sup> and  $\text{Cs}_3\text{EuSi}_6\text{O}_{15}$ .<sup>24</sup>

In summary, the structures of these three lanthanide silicates are based on 1-D silicate chain, 2-D silicate layer, or 3-D silicate framework, which are connected with

$\text{LnO}_n$  polyhedra to form 3-D frameworks. These silicate chain, layer and framework are commonly observed in the existing metal silicates, but the different connections with  $\text{LnO}_n$  polyhedra result in diverse novel structures.

**Photoluminescence properties of TbSiO-CJ8 and EuSiO-CJ8.** It is well-known that microporous lanthanide silicates usually exhibit interesting photoluminescence properties. Here, only the photoluminescence properties of TbSiO-CJ8 and EuSiO-CJ8 synthesized under mild hydrothermal conditions were studied, because they can be obtained as pure phases.

Figure 7a shows the room-temperature (RT) photoluminescence spectrum of TbSiO-CJ8 excited at 267 nm. It shows a series of lines between 450 and 650 nm, which are associated with the  $^5D_4 \rightarrow ^7F_J$  ( $J = 3-6$ ) transitions of  $\text{Tb}^{3+}$  ion. In the spectrum, the green  $^5D_4 \rightarrow ^7F_5$  transitions at 540 and 548 nm are the strongest. But the luminescence from higher excited states (e.g.,  $^5D_3$ ) is not detectable, implying very efficient nonradioactive relaxation to the  $^5D_4$  level. The preliminary study showed that TbSiO-CJ8 is room-temperature green phosphors.

The room temperature emission spectrum of EuSiO-CJ8 with a number of lines between 550 and 750 nm is shown in Figure 7b. These lines are ascribed to the transitions between the first excited  $^5D_0$  state and the  $^7F_{0-4}$  Stark levels of the fundamental  $\text{Eu}^{3+}$  septet. The strongest peak at 591 nm is the red  $^5D_0 \rightarrow ^7F_1$  transition. The emissions from excited levels  $^5D_2$  and  $^5D_1$  were not observed due to efficient nonradioactive relaxation to the  $^5D_0$  levels. The preliminary study showed that EuSiO-CJ8 is room-temperature red phosphors.

## Conclusions

The high-temperature and high-pressure synthetic method has been successfully employed to synthesize three new members of lanthanide silicates with novel 3-D frameworks. All of these compounds contain stoichiometric amounts of lanthanide ions. The structure of GdSiO-CJ7 constructed by zigzag silicate chains and gadolinium chains contains 10-ring channels. TbSiO-CJ8 consists of undulated silicate double layers linked by  $\text{TbO}_6$  octahedron to form a 3-D framework that contains 8-ring channels. DySiO-CJ9 possesses a dense framework containing only 6-rings. The photoluminescence study showed that TbSiO-CJ8 exhibits strong green phosphors. Successively, we will attempt to synthesize the pure phases of GdSiO-CJ7 and DySiO-CJ9 to search for the properties of photoluminescence, ion-exchange, adsorption, etc. The successful synthesis of these three new frameworks under high-temperature and high-pressure hydrothermal conditions will promote further research into lanthanide silicates with novel structures and special properties.

**Acknowledgment.** We thank the National Natural Science Foundation of China (No. 20471022 and 40673051) and the State Basic Research Project of China (Grants 2006CB806103 and 2007CB936402).

**Supporting Information Available:** Figures showing powder XRD patterns and the TGA and crystallographic data in CIF format. This material is available free of charge via the Internet at <http://pubs.acs.org>.

(40) Liebau, F. *Structural Chemistry of Silicates: Structure, Bonding and Classification*; Springer-Verlag: Berlin, 1985.

(41) Donnay, G.; Allmann, R. *Am. Mineral.* **1970**, *55*, 1003.

(42) Chao, G. Y. *Can. Mineral.* **1978**, *16*, 561.

(43) Ghose, S.; Sen Gupta, P. K.; Campana, C. F. *Am. Mineral.* **1987**, *72*, 365.